

**ARE ARTIFICIAL NEURAL NETWORKS THE RIGHT TOOL FOR
MODELING AND CONTROL OF BATCH AND BATCH-LIKE
PROCESSES?**

by

MUSTAFA RASHID, B.Eng

A Thesis

Submitted to the School of Graduate Studies
in Partial Fulfillment of the Requirements for
the Degree Master of Applied Science

MASTER OF APPLIED SCIENCE (2023)
(Chemical Engineering)

McMaster University
Hamilton, Ontario, Canada

TITLE: Are Artificial Neural Networks the Right Tool for Modeling
and Control of Batch and Batch-like Processes?

AUTHOR: Mustafa Rashid, B.Eng
(McMaster University, Hamilton, ON)

SUPERVISOR: Dr. Prashant Mhaskar

NUMBER OF PAGES: ix, 45

ABSTRACT

The prevalence of batch and batch-like operations, in conjunction with the continued resurgence of artificial intelligence techniques for clustering and classification applications, has increasingly motivated the exploration of the applicability of deep learning for modeling and feedback control of batch and batch-like processes. To this end, the present study seeks to evaluate the viability of artificial intelligence in general, and neural networks in particular, toward process modeling and control via a case study. Nonlinear autoregressive with exogeneous input (NARX) networks are evaluated in comparison with subspace models within the framework of model-based control. A batch polymethyl methacrylate (PMMA) polymerization process is chosen as a simulation test-bed. Subspace-based state-space models and NARX networks identified for the process are first compared for their predictive power. The identified models are then implemented in model predictive control (MPC) to compare the control performance for both modeling approaches. The comparative analysis reveals that the state-space models performed better than NARX networks in predictive power and control performance. Moreover, the NARX networks were found to be less versatile than state-space models in adapting to new process operation. The results of the study indicate that further research is needed before neural networks may become readily applicable for the feedback control of batch processes.

ACKNOWLEDGEMENTS

First and foremost, I must extend my sincerest gratitude to my supervisor, Dr. Prashant Mhaskar, who has provided me with invaluable guidance, continuous support, and unending patience throughout my time as his student. I am extremely lucky to have such a caring supervisor whose dedication to his students is inspiring. Dr. Mhaskar persistently went above and beyond the role of a supervisor during the completion of my graduate degree. Thank you, Dr. Mhaskar, for being an exemplary and magnanimous supervisor.

Thank you to McMaster University, the Department of Chemical Engineering and the McMaster Advanced Control Consortium (MACC) for the support that I have received during my graduate degree.

And finally, thank you to my family for their endless support. I am indebted to my parents, whose sacrifices have been critical to where I am today.

Table of Contents

1	Introduction	1
1.1	Motivation	1
1.2	Research Problem Statement	4
1.3	Outline of the Thesis	5
2	Preliminaries	6
2.1	Simulation Example	6
2.2	Subspace Identification	7
2.3	ANN-Based Dynamic Models	10
3	Model Identification	15
4	Closed-Loop Results	26
5	Conclusions and Future Work	36
5.1	Different Systems	37
5.2	Different Neural Network Architectures	37
5.3	Other Methodologies	38
5.4	Process Complexity	38
5.5	Solutions for Addressing Over-fitting	38
5.6	Controller Performance Monitoring	39

List of Figures

3.1	Initial structure from which the architecture of the NARXs was developed.	19
3.2	Structure of NARX networks identified both in the absence and presence of measurement noise.	20
3.3	Validation of state-space models and NARX networks in the absence of measurement noise.	21
3.4	Validation of state-space models and NARX networks subject to measurement noise.	22
3.5	Comparison of input profiles between training (top) and newly generated (bottom) input profiles.	23
3.6	Validation of state-space models and NARX networks in the absence of measurement noise and using distinctly generated input profiles.	24
3.7	Validation of state-space models and NARX networks subject to measurement noise and using distinctly generated input profiles.	25
4.1	Implementation of state-space models and NARX networks into MPC in the absence of measurement noise.	31

4.2	Implementation of state-space models and NARX networks into MPC subject to measurement noise.	32
4.3	Implementation of state-space models and NARX networks into MPC in the absence of measurement noise and using newly generated reference profiles.	33
4.4	Implementation of state-space models and NARX networks into MPC subject to measurement noise and using newly generated reference profiles.	34

List of Tables

2.1	Kinetic mechanism for PMMA polymerization.	6
3.1	Mean NRMSE evaluations for the validation of the identified models.	22
3.2	Mean NRMSE evaluations for the validation of the identified models against distinctly generated input trajectories.	25
4.1	Mean NRMSE evaluations between the control and reference trajectories.	28
4.2	Mean NRMSE evaluations between the control and distinctly generated reference trajectories.	30
4.3	Mean computation times, in seconds, for MPC simulations.	35

Chapter 1

Introduction

1.1 Motivation

Increasing competition and environmental regulations, alongside the importance of batch and batch-like process operation, have impelled manufacturing industries to seek improved margins via optimization of production processes. Several valuable products, including specialty chemicals and bio-pharmaceuticals, are manufactured in batch processes, and advanced process control techniques that utilize process models are being increasingly sought to improve process operation.

All of the diverse modeling techniques can be classified into one of two distinct modeling approaches: first-principles mechanistic-based modeling and empirical data-driven modeling. First-principles models are desired for their ability to capture the underlying mechanics of processes directly through the application of physical conservation laws such as mass or energy balances. However, the development and maintenance of first-principles models remains challenging. As an alternative, the prevalence of historical process data has enabled data-driven modeling to emerge as an attractive alternative.

Myriad modeling methods exist for the purpose of developing models from process

data. Recently, neural networks have yielded compelling results in their ability to handle human tasks such as classification, clustering, pattern recognition, image recognition, and language processing [1]. Neural networks have particularly been shown to be successful in data classification and segmentation tasks [11; 25]. The power of neural networks is evidenced by their wide application, from business and social science to engineering and manufacturing. Neural networks are useful because of their versatility, which allows them to handle non-linear and complex behavior [9]. From the above, it becomes natural to seek to apply neural networks in the context of batch process control. However, the literature remains limited in the application of neural networks toward the development of dynamic models and their use in control in general, and batch process operation in particular.

Instead of neural networks, many statistical modeling approaches are available. One statistical approach is the method of partial least squares (PLS). The PLS method requires data to be partitioned into two matrices: a block for explanatory variables (X) and a block for response variables (Y). PLS is inspired by the methods of multi-linear regression (MLR) and principal component regression (PCR). MLR maximizes the correlation between X and Y ; PCR captures the maximum amount of variance in X through orthogonal linear combinations of the explanatory variables. PLS seeks to consolidate between the aims of both methods by maximizing the covariance between X and Y . PLS achieves this by first projecting the explanatory variables onto a latent variable space to remove collinearity, and then performing linear regression within that latent space [15]. PLS is desired for its ability to handle collinear data and situations in which there are fewer observations relative to the number of explanatory variables. PLS techniques can also be adapted to incorporate first-principles knowledge via appended variables to the data matrices, as calculated by first-principles equations.

An alternative statistical approach is prediction error methods (PEMs). The premise underlying these methods is to determine the model parameters by minimizing the er-

ror between measured and predicted outputs. Constraints can be readily implemented into the optimization so as to impose regularity constraints on model parameters. The advantage of PEM lies in its diverse applicability, as it can be applied to most model structures and can readily handle closed systems. The drawback is the computational cost, as PEM typically requires the solving of non-convex optimization problems.

Yet another popular statistical approach is subspace identification, which identifies state-space models from input/output data. Subspace identification methods comprise of two main steps. The first is to estimate either the extended observability matrix or the state trajectory sequence from a weighted projection of the row space of the Hankel matrices formed from the input/output data. The second step is to then calculate the system matrices [14]. Subspace identification methods are desirable since they are computationally tractable and inherently discourage over-fitting through the use of singular value decomposition (SVD) to estimate the model order.

Recently, artificial neural networks (ANNs) have been championed for the purpose of model identification [22]. The functional form of an ANN is a network of nodes, called neurons, whose values are calculated from a vector of inputs supplied by each neuron in the preceding layer in the network, either the input layer or a hidden layer. Each neuron is connected to all neurons in the previous layer via a weighted connection, essentially leading to a functional form with parameters. The activation in each neuron is calculated as a linear combination of the activations in the previous layer, including a bias, and is modified by an activation function of choice. Common choices for the activation function are the sigmoid, hyperbolic tangent, and rectifier functions.

The networks are trained (i.e., the parameters are determined) by minimizing a cost function with respect to the network parameters, the weights and biases relating each neuron to its preceding layer. To facilitate optimization of the network parameters,

the partial derivatives of the cost function with respect to the network's weights and biases are necessary. The requisite partial derivatives can be calculated by the widely used backpropagation algorithm, which can be conceptualized in two steps. Firstly, the training data are fed to the neural network to calculate the network's outputs and internal activations. Secondly, the needed partial derivatives are calculated backwards, beginning from the output layer, using the chain rule from differential calculus. Finally, the calculated partial derivatives allow for optimization by such methods as gradient descent [29]. While neural networks have generally found widespread acceptance, a comparative study of neural networks with other approaches for batch process modeling and control is lacking.

1.2 Research Problem Statement

In light of the above, the present study aims to address the dearth of results that compare neural networks to other data-driven control techniques for batch processes. Subspace identification, which remains a prevalent and validated modeling approach for batch process control, is used as the comparative benchmark in this work. Due to its dominance in industrial practice, model predictive control (MPC) was chosen as the framework in which the viability of neural networks for control purposes could be evaluated. To carry out the comparison, a batch polymethyl methacrylate (PMMA) polymerization process was selected as the testbed. In particular, the objectives of this research were two-fold:

1. Identification of State-Space and Neural Network Models

Develop state-space and neural network models for the PMMA polymerization process and compare their capacities in modeling the input/output data.

2. Model Predictive Control

Implement both state-space models and neural networks into MPC and compare the control performances gained via each approach.

1.3 Outline of the Thesis

The comparison between the two modeling approaches is illustrated by means of a motivating example which is presented in Section 2.1. Subspace identification and neural networks are explained subsequently in Sections 2.2 to 2.3. Thereafter, Chapter 3 evaluates the models identified and validated per both modeling approaches and Chapter 4 presents the closed-loop results of implementing both types of models into an MPC framework. Finally, concluding remarks and topics for future work are presented in Chapter 5.

Chapter 2

Preliminaries

In this section, we first present an example to motivate our results, followed by a review of existing subspace identification and ANN approaches.

2.1 Simulation Example

Consider a PMMA polymerization process carried out in a batch stirred tank reactor with a heating/cooling jacket. The underlying kinetic mechanism for the free radical polymerization of PMMA is given in Table 2.1, where I is the initiator, M is the monomer, R_i is a live polymer with i monomer units, P_i is a dead polymer with i units, and S is the solvent [32].

Table 2.1: Kinetic mechanism for PMMA polymerization.

Kinetic Mechanism	Chemical Formula
Initiation	$I \rightarrow 2\phi$
	$\phi + M \rightarrow R_1$
Propagation	$R_i + M \rightarrow R_{i+1}$
Termination by combination	$R_i + R_j \rightarrow R_{i+j}$
Termination by disproportionation	$R_i + R_j \rightarrow P_i + P_j$
Chain transfer to monomer	$R_i + M \rightarrow P_i + R_1$
Chain transfer to solvent	$R_i + S \rightarrow P_i + S$

The batch reactor is charged with methyl methacrylate (monomer), AIBN (initiator), and toluene (solvent). The mechanistic model for the motivating example was adapted from [12] while making appropriate alterations as per [13; 32], which are further discussed in [7]. The first-principles model, which is used as a test bed, involves nine states: the concentrations of the monomer and initiator, reactor temperature, and six moments of living and dead polymer chains. The input to the process is the jacket temperature, and the measured outputs are the reaction temperature, the logarithm of viscosity, and density. The plant model was used to generate historical data for the identification of state-space and NARX network models, as well as for producing the process simulation required for model validation and MPC implementation.

2.2 Subspace Identification

Subspace identification techniques identify a linear time-invariant (LTI) state-space model. The deterministic identification problem (for a continuous process) can be described as follows: if s measurements (where s represents the length of the data) of the input $u_k \in \mathbb{R}^m$ and the output $y_k \in \mathbb{R}^l$ are available, then a model with order n can be identified in the form

$$\begin{aligned}x_{k+1}^d &= Ax_k^d + Bu_k \\y_k &= Cx_k^d + Du_k\end{aligned}\tag{2.1}$$

where the objective is to determine the order n of this unknown system and the system matrices $A \in R^{n \times n}$, $B \in R^{n \times m}$, $C \in R^{l \times n}$, $D \in R^{l \times m}$.

We denote the measured outputs as $y^{(b)}[k]$, where k is the sampling time from when the run is initialized and b denotes the run number. Thus, the Hankel matrix is laid out as follows:

$$Y_{1|i}^{(b)} = \begin{bmatrix} y^{(b)}[1] & y^{(b)}[2] & \cdots & y^{(b)}[j^{(b)}] \\ \vdots & \vdots & & \vdots \\ y^{(b)}[i] & y^{(b)}[i+1] & \cdots & y^{(b)}[i+j^{(b)}-1] \end{bmatrix} \quad \forall b = 1, \dots, nb \quad (2.2)$$

where nb is the total number of runs used for identification.

A single Hankel matrix by itself would not allow data from multiple experiments or runs to be utilized, and the simple concatenation of the outputs from all of the runs would generate a data set where the initial condition of a subsequent run is the end point of the previous run, which would also be incorrect. Therefore, when concatenating the data, it is important to generate a matrix where this assumption is not necessary to solve for the states. This can be achieved by horizontally concatenating the Hankel matrices from each run to generate our pseudo-Hankel matrix for both the input and output variables. This pseudo-Hankel matrix for the output data is defined as follows:

$$Y_{1|i} = \begin{bmatrix} Y_{1|i}^{(1)} & Y_{1|i}^{(2)} & \cdots & Y_{1|i}^{(nb)} \end{bmatrix} \quad (2.3)$$

Similarly, a pseudo-Hankel matrix for the input data can be generated. A key consideration of this approach is that horizontal concatenation of data allows for runs of varying lengths to be identified without aligning the variables. The use of these pseudo-Hankel matrices for input and output data allows for multiple runs to be analyzed to compute the state trajectory using any subspace identification technique, such as the deterministic method used in this approach [27]. A consequence of horizontal concatenation is that the identified state trajectories also consist of horizontally

concatenated state estimates from each run, which can be represented as

$$\hat{X}_{i+1}^{(b)} = \left[\hat{x}^{(b)}[i+1] \quad \cdots \quad \hat{x}^{(b)}[i+j^{(b)}] \right] \quad \forall b = 1, \dots, nb \quad (2.4)$$

$$\hat{X}_{i+1} = \left[\hat{X}_{i+1}^{(1)} \quad \hat{X}_{i+1}^{(2)} \quad \cdots \quad \hat{X}_{i+1}^{(nb)} \right] \quad (2.5)$$

where nb is the total number of training runs used for identification. Finally, once the state trajectory matrix is determined, the system matrices can be estimated using such methods as ordinary least squares, as shown below:

$$Y_{reg}^{(b)} = \begin{bmatrix} \hat{x}^{(b)}[i+2] & \cdots & \hat{x}^{(b)}[i+j^{(b)}] \\ y^{(b)}[i+1] & \cdots & y^{(b)}[i+j^{(b)}-1] \end{bmatrix} \quad (2.6)$$

$$X_{reg}^{(b)} = \begin{bmatrix} \hat{x}^{(b)}[i+1] & \cdots & \hat{x}^{(b)}[i+j^{(b)}-1] \\ u^{(b)}[i+1] & \cdots & u^{(b)}[i+j^{(b)}-1] \end{bmatrix} \quad (2.7)$$

$$\begin{bmatrix} Y_{reg}^1 & \cdots & Y_{reg}^{(nb)} \end{bmatrix} = \begin{bmatrix} A & B \\ C & D \end{bmatrix} \begin{bmatrix} X_{reg}^{(1)} & \cdots & X_{reg}^{(nb)} \end{bmatrix} \quad (2.8)$$

yielding A , B , C and D as the state-space model matrices, which are henceforth collectively referred to as the unconstrained model.

Remark 1. *The key consideration for subspace identification of multiple data sets, as opposed to a single data set, is in the generation of the state trajectory. The risk of not using a pseudo-Hankel matrix structure through a concatenation of the data can result in a single-state trajectory for the data set, where the initial point of the next run is incorrectly linked to the end point of the previous run. The subspace identification approach allows for the correct identification of the separate state trajectories from the training data to be used for model identification, thus enabling the usage of multiple*

runs during training.

Notably, prior work has assessed the value of subspace identification for batch processes [8]. Subspace identification was employed to generate a data-driven state-space model for the PMMA polymerization process being used as a test-bed for the present study. The state-space model was then implemented into MPC and the resulting performance was compared with state-of-the-art latent variable methods. The results from their investigation demonstrated the superiority of using subspace identification for the modeling and control of batch processes. Motivated by these findings, state-space models were selected as the benchmark by which to evaluate ANNs in this work.

2.3 ANN-Based Dynamic Models

To enable the modeling of dynamical systems in ANNs, information is allowed to flow between each iteration via tapped delay lines or recurrent (feedback) connections. For instance, time delay neural networks are feedforward dynamic neural networks that allow for the inclusion of historical data via tapped delay lines.

Recurrent neural networks (RNNs), however, are more suitable for dynamic process modeling, as they encode an internal state (memory) of the system by incorporating feedback connections. Past outputs or hidden states are looped back into the neural network, thereby allowing for information to flow between each iteration of the network. Hence, the response of RNNs depends on the historical sequences of both input and output data. NARX networks, a class of RNNs involving only feedback from the output neuron, are used as a representative for this study [33]. A mathematical representation of a general NARX network is given by

$$y(n+1) = f[y(n), \dots, y(n-d_y); u(n), \dots, u(n-d_u)] \quad (2.9)$$

where $u(n)$ and $y(n)$ are the current inputs and outputs, $d_u(n)$ and $d_y(n)$ are the associated input and output delays, and $f(\cdot)$ is a non-linear function [5].

NARX networks are derived from the application of autoregressive exogenous (ARX) models to the framework of artificial intelligence. Therefore, NARX networks are the artificial intelligence counterparts of ARX models, which are a mainstay of process modeling. Contrasting the two modeling approaches, it is noteworthy that far more advanced computational techniques have been developed for neural networks than exist for traditional ARX modeling. In particular, NARX networks can readily incorporate nonlinear elements via a host of different activation functions.

RNNs are able to learn temporal sequences by retaining a "memory" of system dynamics. However, practice reveals that RNNs are difficult to train, particularly in learning dependencies over long sequences of data [34]. The difficulties in training RNNs can be understood by looking carefully at their associated learning algorithms. To optimize the cost function, the algorithm of back propagation through time (BPTT) is used. In BPTT, the RNN is first 'unrolled' across a time sequence before the regular backpropagation algorithm can be used for optimization purposes. Hence, BPTT is simply a specific application of backpropagation to the learning of RNNs. Since the unrolled RNN often becomes very deep, the training of RNNs is especially complicated by the problem of exploding or vanishing gradients. For this reason, RNNs struggle to store information over extended time intervals [19].

LSTM networks have been proposed as an alternative to RNNs. LSTM networks are a class of RNNs whose architecture incorporates long-term memory over extended time intervals via the inclusion of a cell state. The cell state is updated at each time step via forget and input gates while the hidden state (the short-term memory state

of RNNs) is controlled by an output gate. LSTM networks effectively mitigate the vanishing gradient problem by maintaining constant error backpropagation via the cell state [19].

In light of the above, LSTM networks have become a popular class of RNNs for a variety of applications, such as speech recognition, translation, and language modeling. However, for the purposes of dynamic systems modeling in the framework of model-based control, the value of LSTM networks remains to be established. The main advantage of LSTM networks is the ability to learn long-term dependencies in sequential data. However, for dynamic models, the output at any given time step is largely a function of recent input and output data; the contribution of historical data reaching far back in time will attenuate over lengthy time intervals. Moreover, while learning such long-term dependencies holds the promise of more nuanced modeling, the drawback remains that over-fitting is likely to remain a problem. This is one of the reasons why state-space models have become a mainstay in model-based control, as they provide simpler but stable models which are robust to over-fitting.

Finally, it is noteworthy that [40] found that NARX networks outperformed LSTM networks and convolutional neural networks in predicting groundwater level forecasts. Based on these considerations, NARX networks were selected for the architectures of the ANNs in this work.

The use of ANNs in a framework of MPC has been explored in some contexts. For example, ANN-based MPC of constrained non-linear systems [3] was proposed, where the ANN was trained by minimizing an MPC cost function. An ANN-MPC formulation was also augmented with a second ANN that would adaptively update the identified model online [18]. Another approach was to design an ideal MPC, and then train LSTM networks on the generated control sequences to replace the MPC framework altogether, thereby circumventing computationally expensive optimiza-

tion solutions [24]. LSTM networks have also been implemented for the extraction of phase-specific features in batch processes in order to decrease the overall dimensionality of the prediction scheme [36]. Moreover, LSTM networks have been applied to develop reinforcement learning controllers for enhancing the performance of heating ventilation and air conditioning systems [37].

Another approach is to include first-principles knowledge of the process via weight constraints on the training of RNNs or through the pruning of neuronal connections [39]. It was demonstrated that such physics-based modifications to the RNNs resulted in an improved control performance. Similarly [4] incorporated a priori physical knowledge into RNNs to improve the RNN-based MPC performance of large-scale and complex chemical processes. The application of RNNs toward MPC despite the problem of collinear or insufficiently rich input data [17] was also recently addressed. Their proposed solution was to first use PCA to eliminate collinearity in the input space before identifying an RNN based on the uncorrelated scores.

Among recent developments in the field, [21] compared first-principles, state-space, and ANN models in an economic MPC framework. The authors found that the ANNs often returned non-smooth prediction trajectories that complicated the solution of the optimization problem. In another study, [2] was able to attain optimal or near-optimal control of irrigation schedules by implementing an LSTM network in a mixed-integer MPC scheme. Their contributions warrant further exploration of ANNs for the modeling and control of processes with continuous inputs. Finally, [10] used LSTM networks to develop reduced-order state estimators for mechanistic models of high computational complexity.

Lastly, it must be noted that prior studies in the field have sought to examine the value of ANNs for batch process modeling and control. For example, [38; 31; 23; 35; 28; 41; 20] implemented ANNs for process modeling and control. However, past re-

search has either failed to benchmark ANNs or compared the use of ANNs to classical proportional–integral–derivative control or first-principles mechanistic model-based control. As such, the comparison of ANNs to other data-driven modeling techniques, such as subspace-based state-space models, remains sparse in the literature, despite subspace identification-based models having been shown to be particularly effective in batch control [8]. Therefore, the present study seeks to address this gap by providing a comparison between subspace models and ANNs in the context of model-based predictive control of batch processes.

Chapter 3

Model Identification

The first step in the proposed approach was to identify both (LTI) state-space models and NARX networks for the PMMA polymerization process. To facilitate a comprehensive comparison between the state-space and NARX network models, data sets were built using different input profiles. In particular, three distinct types of input profiles were used to generate the data sets from which the models were identified. The three types of input profiles were formed by implementing three different kinds of input profiles on the PMMA polymerization process. Specifically, the input profiles were as follows:

1. A proportional–integral controller was used to track set-point trajectories.
2. A pseudo-random binary sequence (PRBS) signal was superimposed onto the input moves generated by a proportional–integral controller.
3. A PRBS signal was superimposed onto a nominal input trajectory.

A major aim of this study was to detect and compare over-fitting issues between subspace and NARX network models. To this end, two different sets of historical data were used to identify all models: data both with and without measurement noise. To generate noisy data, Gaussian noise was superimposed onto all output data. Specifically, measurement noise was generated from standard normal distributions modified

by factors of 0.10 for temperature, 0.01 for $\log(\text{viscosity})$, and 0.10 for density. Hence, each model was identified and evaluated for performance both in the presence and absence of noise. In this way, state-space and NARX network models were compared in their robustness to over-fitting issues resulting from noisy data.

The identification of ANNs is complicated by inherent randomness in the training algorithms. Randomness is introduced in the training of ANNs via random parameter initialization and sampling division, among other sources [26]. Such randomness in the training process often leads to a lack of replicability in model identification. To ensure replicability and consistency, the seed was set to a specific and definite value, thereby permitting consistent comparisons between state-space models and NARX networks. However, it is noteworthy that neural networks will often perform differently depending on the seed. A possible explanation for this observation can be the existence of multiple local minima on the surfaces of the cost function. For this reason, it has been suggested to include the seed as a hyperparameter in the identification of neural networks [6].

The models were fitted against training data, and goodness-of-fit evaluations were calculated as per the normalized root mean squared error (NRMSE) measure, given by

$$NRMSE(i) = \frac{\|y_{ref}(:, i) - y(:, i)\|}{\|y_{ref}(:, i) - \text{mean}(y_{ref}(:, i))\|} \quad (3.1)$$

where y is the predicted output, y_{ref} is the measured output, and i indexes the outputs. For the NRMSE evaluation, zero indicates a perfect fit, unity indicates that the model is no better than a straight line in explaining the variance of the data, and a large value indicates a poor fit.

Three sets of historical data were generated for model identification. Each data set

comprised of thirty batches, ten batches for each of the three types of input profiles listed above. The first of these data sets was used as training data to identify the initial state-space models and NARX networks; the associated NRMSE calculations yielded the fit of the models. The identified models were then evaluated for predictive power against a second data set, with the NRMSE calculations being taken as an internal validation of the models. The models were then tweaked for improved performance by trial-and-error optimization of the NRMSE evaluations with respect to model parameters, for cases both with and without measurement noise.

However, the goodness-of-fit of a model does not preclude the possibility of overfitting. Hence, an approach as described would be naive and insufficient for accurately assessing the predictive power of models. Consequently, it is essential to validate the models against novel data. For this reason, an additional measure of the models was calculated. In this last step, the tweaked models were validated against a third set of data. Finally, these resulting NRMSE evaluations were taken as the validation and true measures of model performance.

The procedure described above was followed in the identification of state-space models. The parameter for the number of states ($n = 10$) was tuned by a brute-force search that yielded the best fit, or the best NRMSE evaluation, in comparing model predictions to training data. The lag i was set to twice the number of states. The identified state-space models were tested against the second set of data for the purpose of internal validation. The associated NRMSE calculations were used to tweak model parameters for improved performance; however, this step was found to be unnecessary for state-space models. Finally, the state-space models were validated against the last set of data; the resulting NRMSE calculations were considered the true measures of the models' predictive power.

In the validation of state-space models, Kalman filters were used for state estimation.

The equations for the Kalman filter are given in Equation (3.2), where $P_{k|k-1}$ is the estimated (a priori) covariance, $P_{k|k}$ is the estimated (a posteriori) covariance, and K_k is the Kalman gain; Q and R , calculated as per Equation (3.3), are the covariance matrices for both the process and measurement noise, respectively. The two covariance matrices are taken to be time independent.

$$\begin{aligned}
 P_{k|k-1} &= AP_{k-1|k-1}A^T + Q \\
 K_{k|k} &= \frac{P_{k|k-1}C^T}{CP_{k|k-1}C^T + R} \\
 P_{k|k} &= (I - K_k C)P_{k|k-1} \\
 \hat{x}_{k|k-1} &= A\hat{x}_{k-1|k-1} + Bu_k \\
 \hat{x}_{k|k} &= \hat{x}_{k|k-1} + K_k[y_k - (C\hat{x}_{k|k-1} + Du_k)] \\
 \hat{y}_{k|k} &= C\hat{x}_{k|k} + Du_k
 \end{aligned} \tag{3.2}$$

$$\begin{aligned}
 Q &= \text{cov}(X_{k+1} - [A \ B][X_k \ U_k]^T) \\
 R &= \text{cov}(Y_k - [C \ D][X_k \ U_k]^T)
 \end{aligned} \tag{3.3}$$

The initial state estimate was set as the zero vector and the initial Kalman gain was set as the zero matrix. To ensure convergence, the Kalman filter was allowed to run iteratively until the absolute values of the observation error for each output fell below a threshold, as given in Equation (3.4). These threshold values were tuned via trial-and-error until acceptable convergence was achieved. The first ten data samples were discarded in all NRMSE calculations to allow for the observer to converge.

$$|Y_k - \hat{Y}_k| < [0.3 \ 0.1 \ 0.5]^T \quad (3.4)$$

NARX networks were identified following a similar procedure as for state-space models. Firstly, the NARX networks were trained on the first set of data. In the training of all NARX networks, 70% of the input/output data were reserved for training, 15% for validation, and 15% for testing. For all NARX networks, outputs and errors were normalized within the ranges of $(-0.5, 0.5)$ and $(-1, 1)$ respectively. The initial, rudimentary architecture from which neural networks were developed is shown in Figure 3.1. The neural transfer functions, number of hidden layers, and size of the hidden layers were determined by trial-and-error until the best NRMSE evaluation was found.

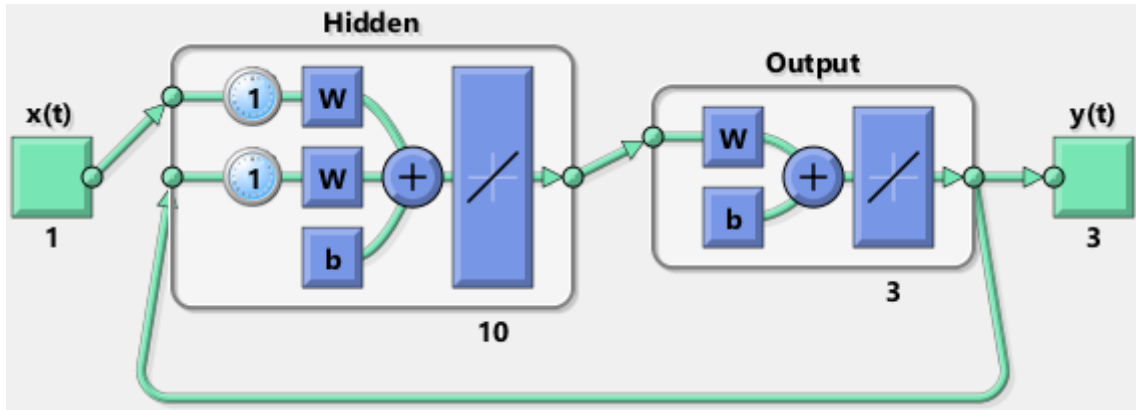


Figure 3.1: Initial structure from which the architecture of the NARXs was developed.

Then, the trained networks were internally validated against a second set of input/output data; the model parameters and architectures were tweaked by a trial-and-error approach. Lastly, the neural networks were validated against the third and final set of data to obtain NRMSE calculations representing the true model performance of the networks. Figure 3.2 displays the final architecture of the neural networks

identified, both in the absence and presence of measurement noise.

Notably, the first layer of the NARX network incorporates an initial nonlinear element to capture the nonlinear dynamics of the PMMA polymerization process. As discussed earlier, one of the main advantages of ANNs over state-space models is in their ability to handle nonlinearities directly. By including nonlinearity into the model, ANNs allow for the enhanced assimilation of process knowledge and thereby strive to improve predictive and control performance.

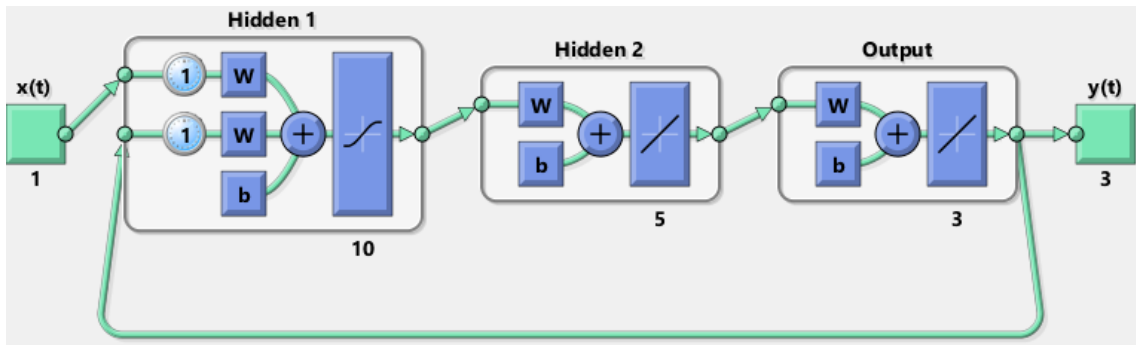


Figure 3.2: Structure of NARX networks identified both in the absence and presence of measurement noise.

Note that while the neural networks do not require an explicitly designed observer as do state-space models, an initial fragment of the input/output data is required to initialize the NARX networks, as is the case for ARX models in general. This initial fragment of input/output data needed by NARX networks can be thought of as representing the role of a state-space observer, with the length of data reflecting the time it would take for the state-space observer to converge to an accurate state estimate.

Table 3.1 tabulates the NRMSE evaluations associated with the validation of both state-space models and NARX networks. Accordingly, Figures 3.3 and 3.4 display an example of the validation of state-space models and NARX networks, identified

both in the absence and presence of measurement noise, respectively. The state-space models outperformed NARX networks in predictive power, as observed by the lower NRMSE evaluations for state-space models in Table 3.1. The data also reveal that both state-space models and NARX networks were resilient to over-fitting measurement noise since the NRMSE evaluations did not increase sharply upon incorporation of measurement noise.

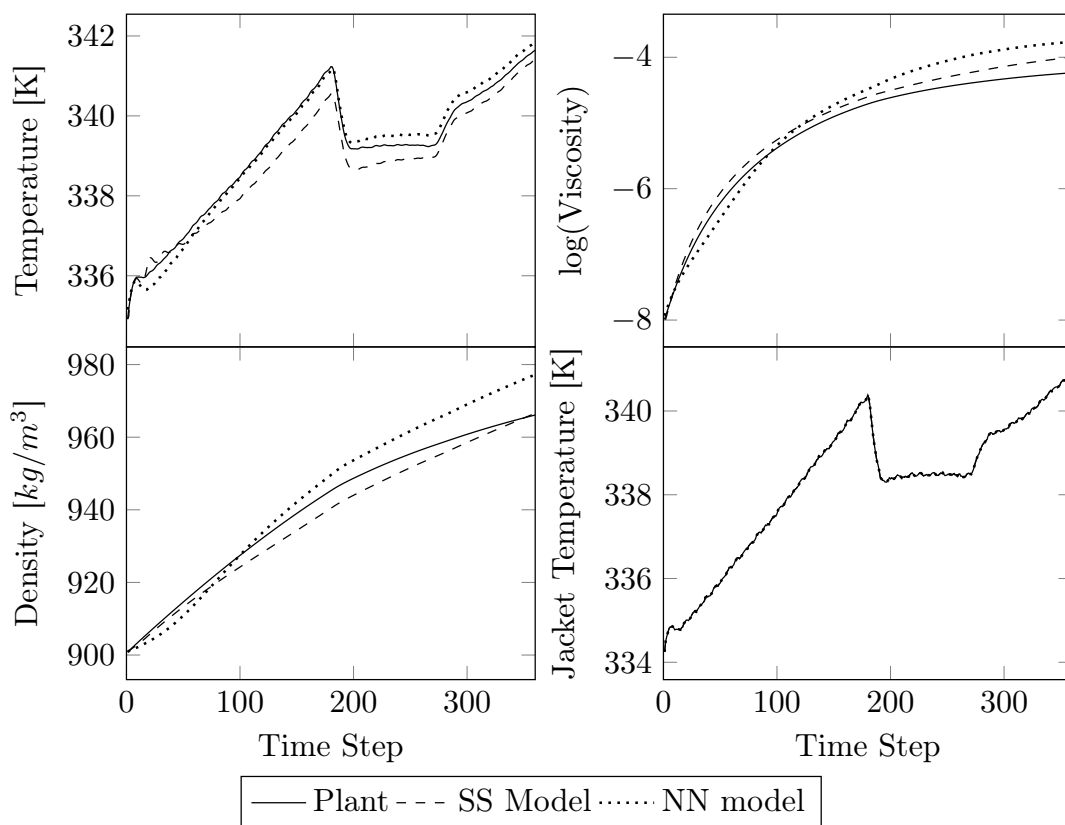


Figure 3.3: Validation of state-space models and NARX networks in the absence of measurement noise.

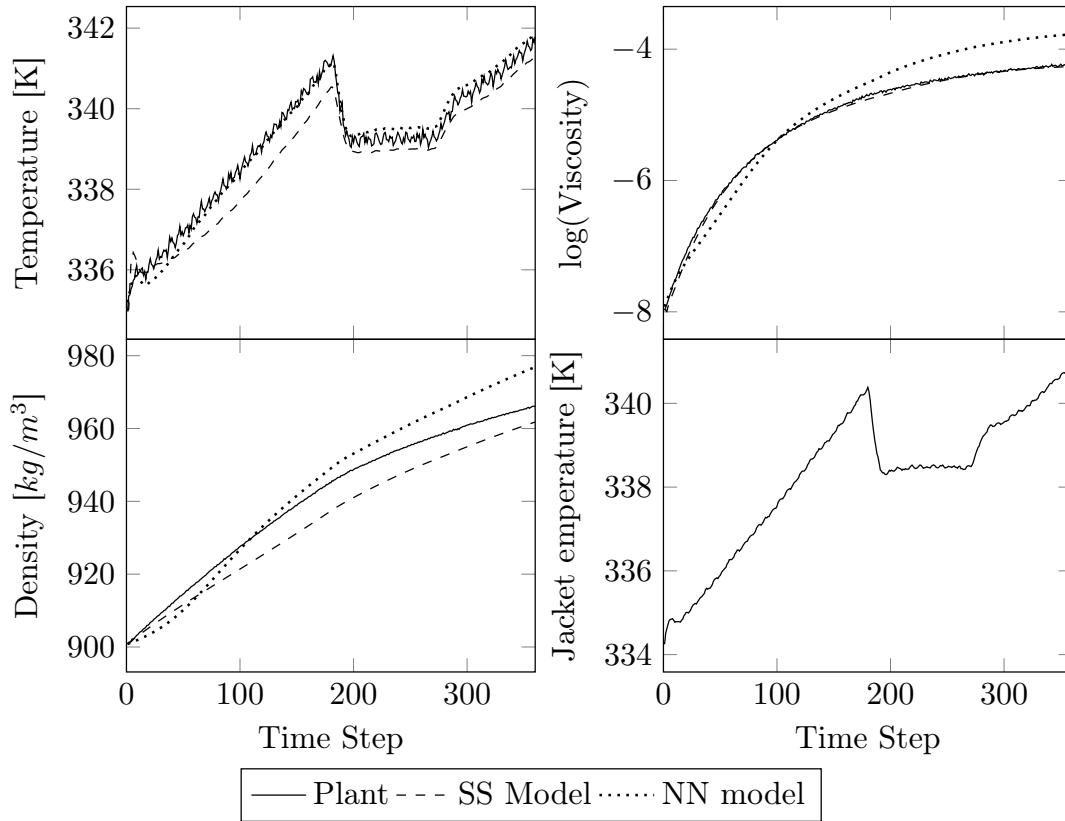


Figure 3.4: Validation of state-space models and NARX networks subject to measurement noise.

Table 3.1: Mean NRMSE evaluations for the validation of the identified models.

	Temperature [K]	log(Viscosity)	Density [kg/m ³]
State Space (without measurement noise)	0.19	0.08	0.08
State Space (with measurement noise)	0.23	0.08	0.10
NARX network (without measurement noise)	0.27	0.21	0.23
NARX network (with measurement noise)	0.29	0.22	0.23

To further assess model performance, the identified models were tested against a fourth set of historical plant data. For the purposes of gauging possible over-fitting, this new set of data was generated to be distinct from the three types of data sets

used previously in model identification. In particular, the data set was formed via the generation of PRBS input profiles. Figure 3.5 contrasts between one of the input profiles used in model identification and one of the input profiles from this fourth data set.

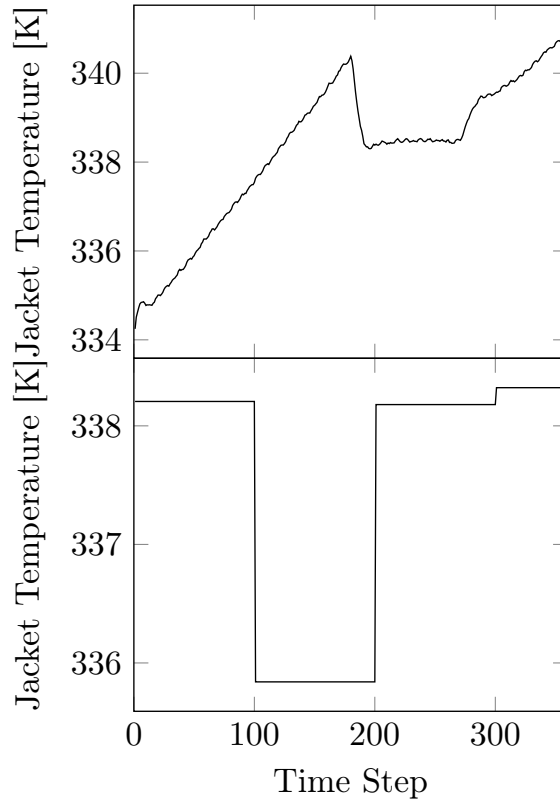


Figure 3.5: Comparison of input profiles between training (**top**) and newly generated (**bottom**) input profiles.

Table 3.2 tabulates the mean NRMSE evaluations associated with the plant data and model predictions. Concurrently, Figures 3.6 and 3.7 present examples of prediction performance for the identified models. Here, a large performance gap is observed between the predictive power of state-space models and NARX networks, as observed by the increased difference between NRMSE evaluations between the modeling approaches. NARX networks are shown to be poor in predicting new and distinct data profiles. While the neural networks did not significantly over-fit measurement noise,

as was established earlier, they did over-fit the training data. This is clearly evidenced by the worse NRMSE evaluations for NARX networks modeling input/output data that are characteristically distinct from the original training data.

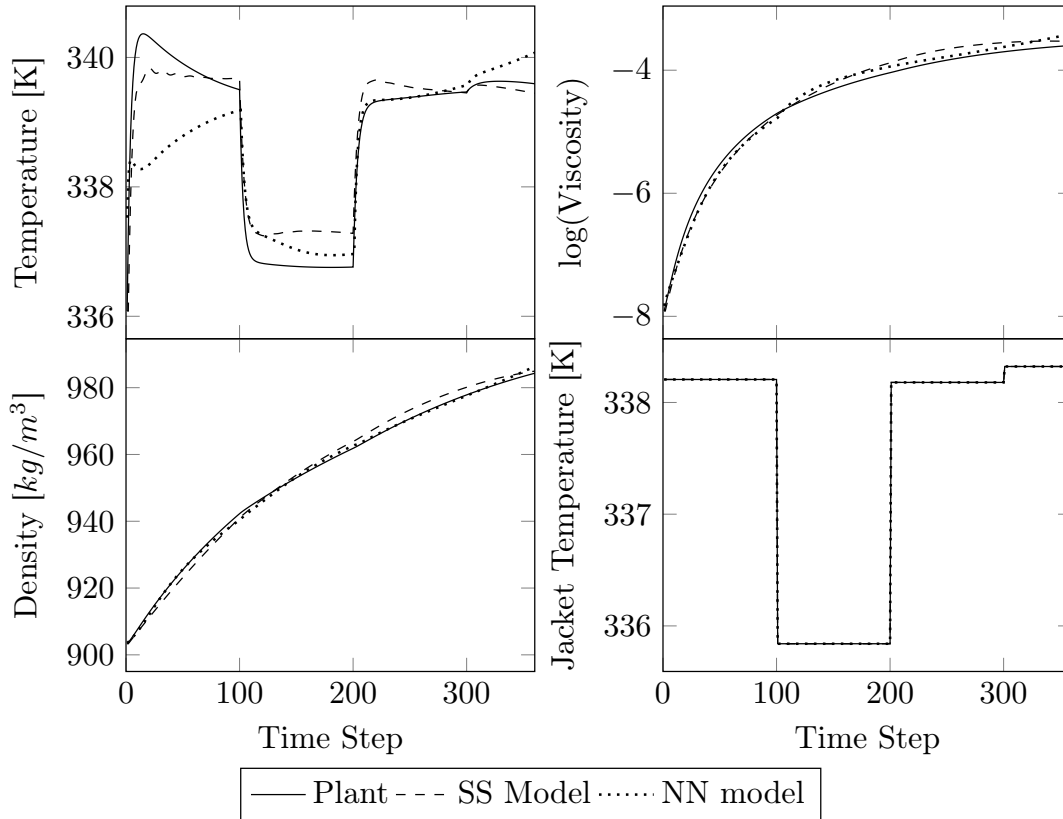


Figure 3.6: Validation of state-space models and NARX networks in the absence of measurement noise and using distinctly generated input profiles.

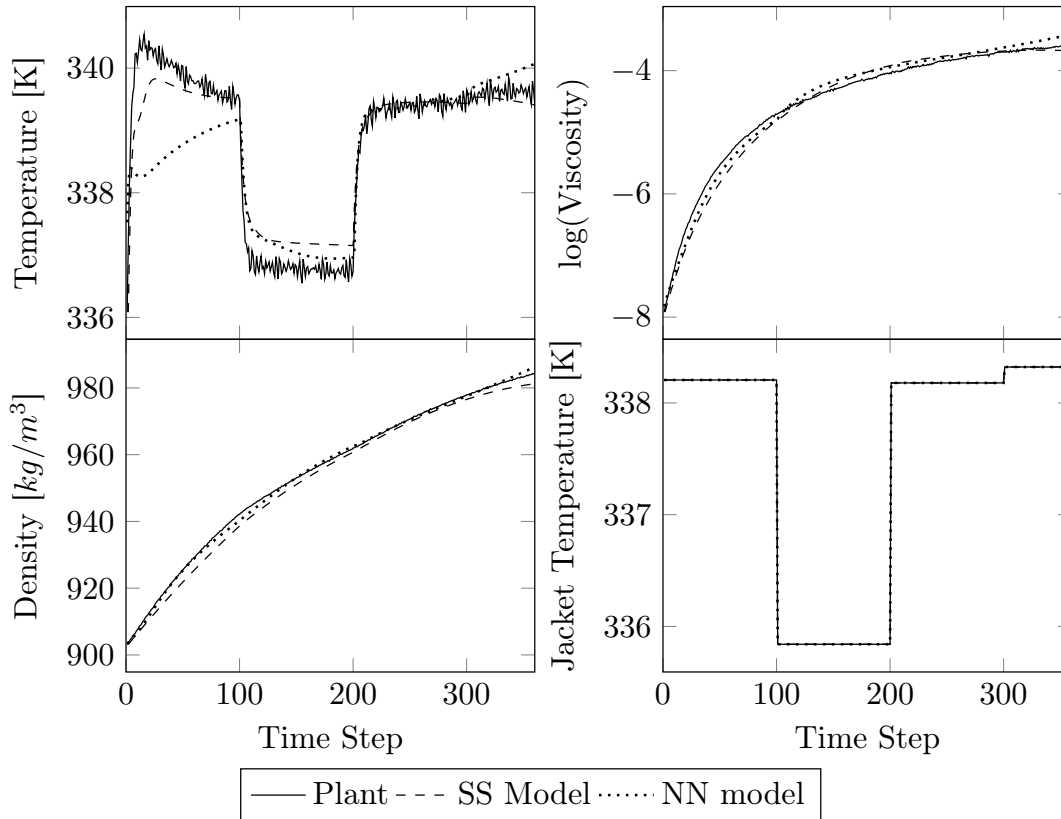


Figure 3.7: Validation of state-space models and NARX networks subject to measurement noise and using distinctly generated input profiles.

Table 3.2: Mean NRMSE evaluations for the validation of the identified models against distinctly generated input trajectories.

	Temperature [K]	log(Viscosity)	Density [kg/m ³]
State Space (without measurement noise)	0.20	0.13	0.09
State Space (with measurement noise)	0.20	0.14	0.12
NARX network (without measurement noise)	0.52	0.30	0.33
NARX network (with measurement noise)	0.52	0.30	0.33

Chapter 4

Closed-Loop Results

Having identified both state-space models and NARX networks, the models were then implemented into MPC for forward prediction of the evolution of the PMMA polymerization process. The control structure of the MPC was such that the jacket temperature (input) was used to control the reactor temperature, logarithm of viscosity, and density (outputs). The MPC scheme was realized by minimizing the cost function

$$\begin{aligned} J &= \sum_{i=1}^{H_p} dy(i) \times Q_y \times dy(i)^T + du(i) \times R_{du} \times du(i)^T \\ dy(i) &= y(i) - y_{ref}(i) \\ du(i) &= u(i) - u(i-1) \end{aligned} \tag{4.1}$$

where R_{du} and Q_y are positive definite weighting matrices penalizing input moves and deviation from the reference output trajectory, respectively. MPC was implemented in MATLAB using the *fmincon* function; iteratively, at each time step, the *fmincon* solver was called to solve the optimization problem for the optimal control moves.

In the case of state-space models, the MPC parameters were tuned such that Q_y was set to the identity matrix, R_{du} was set to the zero matrix, and $H_p = H_c = 1$ was set as

both the prediction and control horizons. Additionally, a Kalman filter was repeated as similar to Chapter 3, except that the initial state vector was now estimated using MATLAB's *findstates* function from training data.

As with ARX models, it is necessary to initialize the internal states of the (closed-loop) NARX networks at each time step to allow for forward prediction. To achieve this, recent plant data were used to iteratively update the internal states of the NARX networks; this can be thought of as being analogous to how state estimation is implemented in the use of state-space models. In particular, the last 10 time steps of input/output data were used to initialize the neural network at each iteration.

In the case of neural networks, the MPC parameters were picked as follows: $Q_y = \begin{pmatrix} 100 & 0 & 0 \\ 0 & 1 & 0 \\ 0 & 0 & 1 \end{pmatrix}$, $R_{du} = 50$, $H_p = 2$ was set as the prediction horizon, and $H_c = 1$ the control horizon. For the first 10 time steps, the plant was allowed to operate under open-loop conditions. Then, closed-loop control was implemented using the NARX networks as predictors for the MPC. At each iteration, the last 10 time steps were used to estimate the current internal state of the neural network.

Remark 2. *An important consideration is that the controllers for the state-space models and NARX networks, which were tuned by trial-and-error for performance, are different. Accordingly, the control performance depends on not only model performance, but also on the suitability of the tuning parameters. However, it is not trivial to separate and identify the specific impacts of the model's predictive performance and the controller's tuning parameters. One possibility would be to examine the control performance of both state-space models and NARX networks under a range of controllers whose parameters have been selected randomly. Another possibility would be to implement both state-space models and NARX networks on two different controllers: one that has been tuned for state-space models and another that has been tuned for the NARX networks. These explorations remain the subject of future work.*

Table 4.1 compares the mean errors over all three process outputs in applying MPC using both state-space models and NARX networks. Both types of models were implemented in MPC, and several tests were run for 10 different reference trajectories, which were in turn determined from each of the three types of input profiles as from Chapter 3.

Errors between the control and reference trajectories were evaluated via NRMSE calculations; the means of those NRMSE calculations over all 30 implementations are given in Table 4.1. State-space models outperformed NARX networks in control of temperature, the output exhibiting the most non-linear behavior; both models provided almost identical control over the other outputs. The control performance of NARX networks deteriorated more due to noisy conditions than that of state-space models. Figures 4.1 and 4.2 show examples of the implementation of state-space and NARX network models in MPC.

Table 4.1: Mean NRMSE evaluations between the control and reference trajectories.

	Temperature [K]	log(Viscosity)	Density [kg/m ³]
State Space (without measurement noise)	0.49	0.61	0.56
State Space (with measurement noise)	0.56	0.61	0.56
NARX network (without measurement noise)	0.60	0.60	0.58
NARX network (with measurement noise)	1.07	0.60	0.58

To further assess model performance, the identified models were used to track novel reference trajectories. For the purposes of gauging over-fitting, this new set of data was generated to be distinct from the data sets used previously in model identification and validation. As discussed in Chapter 3, the data set was formed via the generation of PRBS input profiles. Refer back to Figure 3.5 to see an example comparison between one of the input profiles used in model identification and one of the input profiles from this final data set.

Table 4.2 tabulates the mean NRMSE evaluations associated with the plant data and model predictions. State-space models and NARX networks provided similar control performance for the log(viscosity) and density outputs. Additionally, neither model was heavily impacted by measurement noise. However, there was a significant gap between the two modeling approaches in the control of temperature. Therefore, it is concluded that state-space models outperformed NARX networks in the control of novel reference trajectories. The data indicate that NARX networks were less versatile than state-space models in generalizing beyond the range of training data. Figures 4.3 and 4.4 present a visual comparison between the prediction performance of both modeling approaches with regards to novel data.

Table 4.2: Mean NRMSE evaluations between the control and distinctly generated reference trajectories.

	Temperature [K]	log(Viscosity)	Density [kg/m³]
State Space (without measurement noise)	0.05	0.01	0.00
State Space (with measurement noise)	0.18	0.02	0.01
NARX network (without measurement noise)	0.58	0.04	0.02
NARX network (with measurement noise)	0.67	0.04	0.03

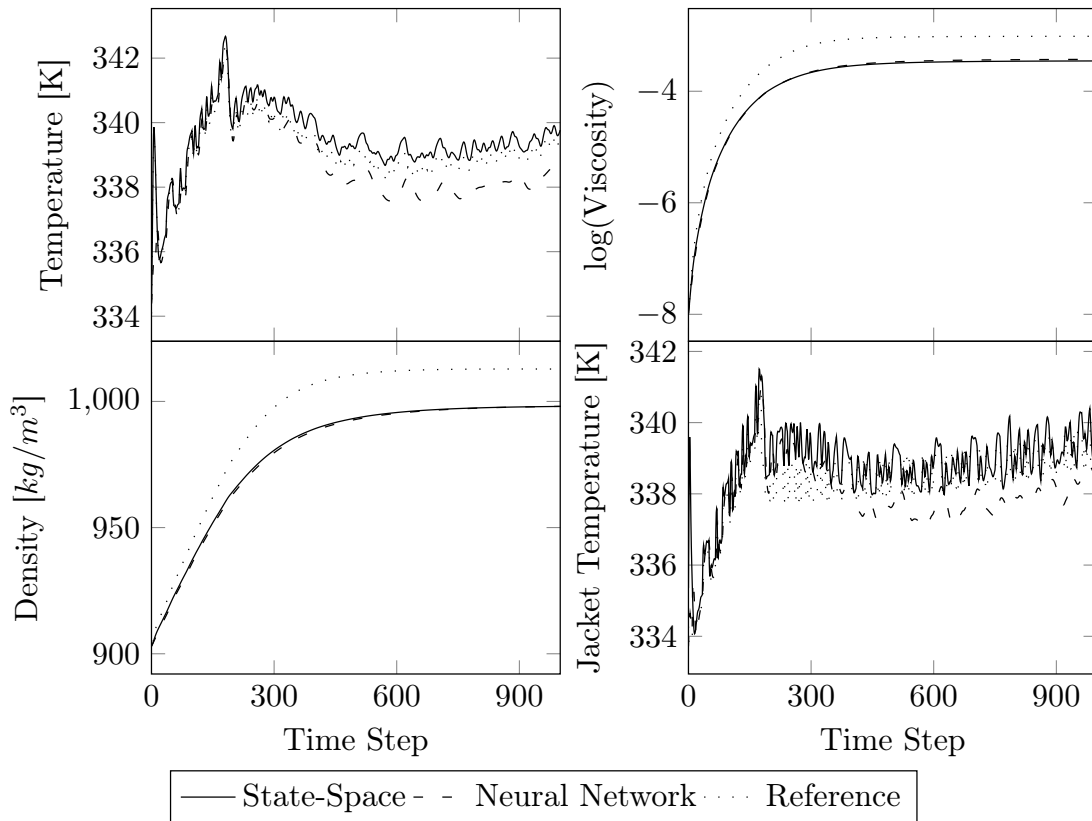


Figure 4.1: Implementation of state-space models and NARX networks into MPC in the absence of measurement noise.

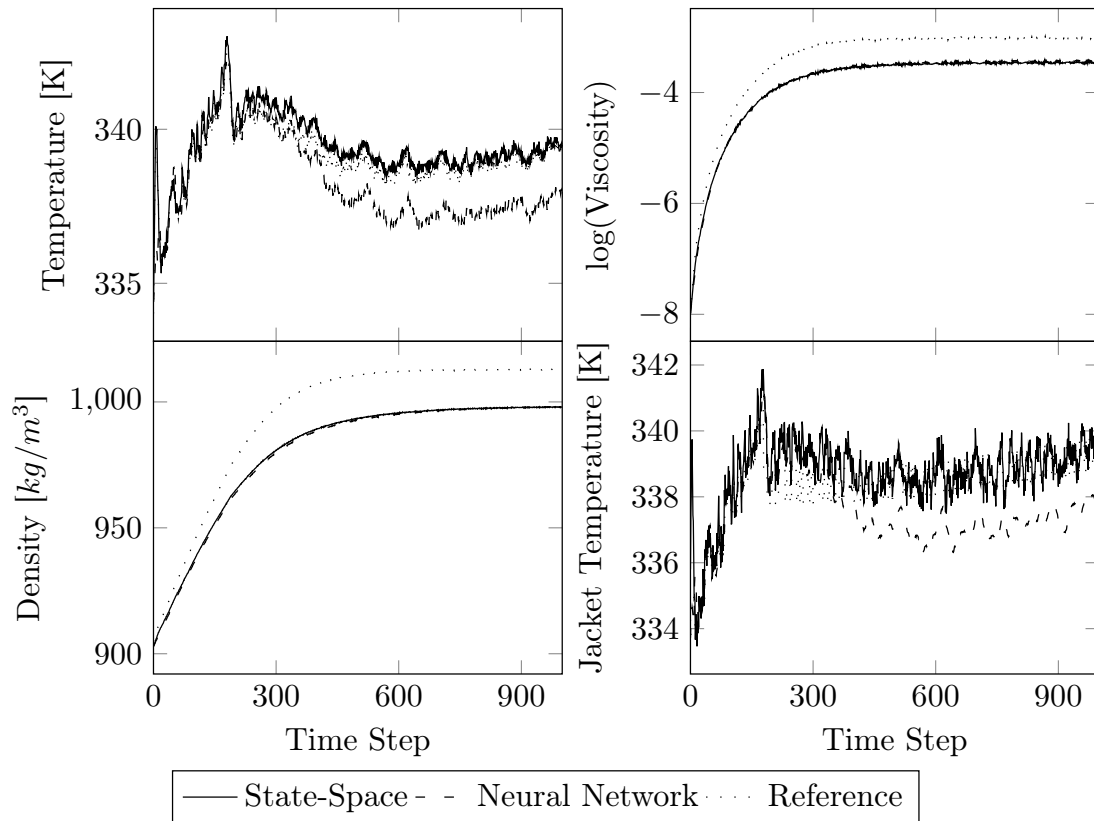


Figure 4.2: Implementation of state-space models and NARX networks into MPC subject to measurement noise.

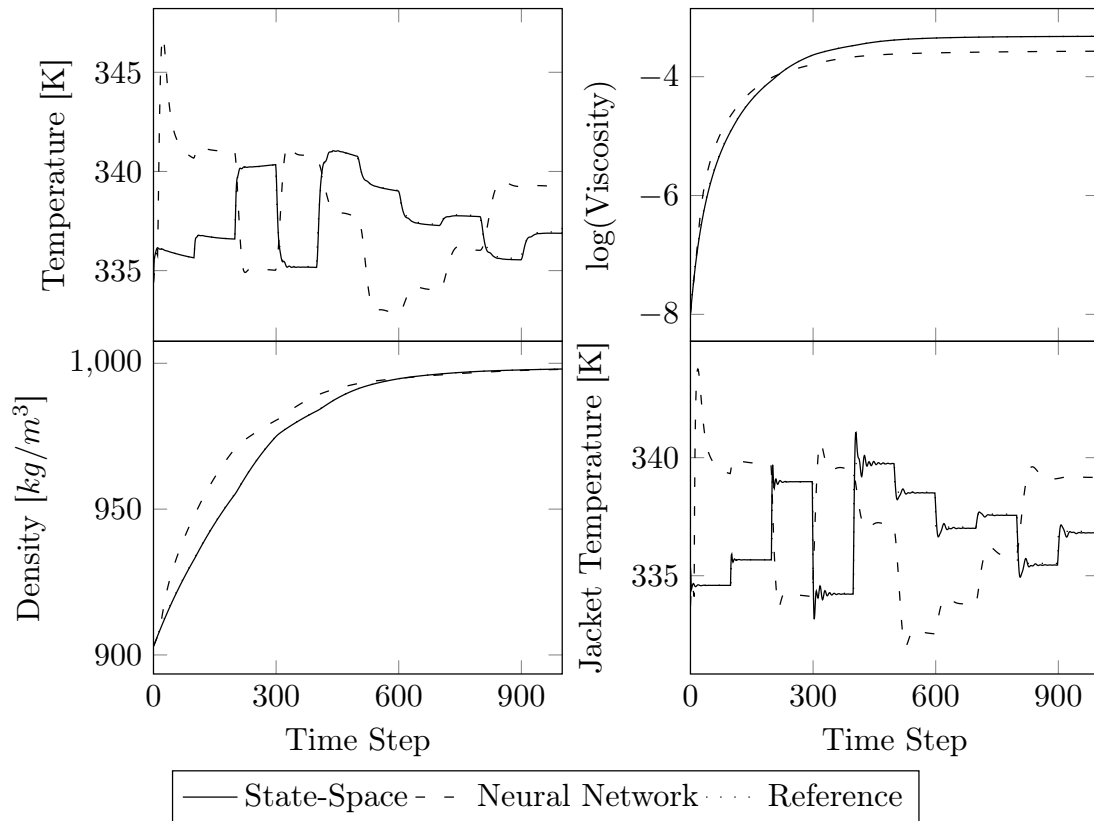


Figure 4.3: Implementation of state-space models and NARX networks into MPC in the absence of measurement noise and using newly generated reference profiles.

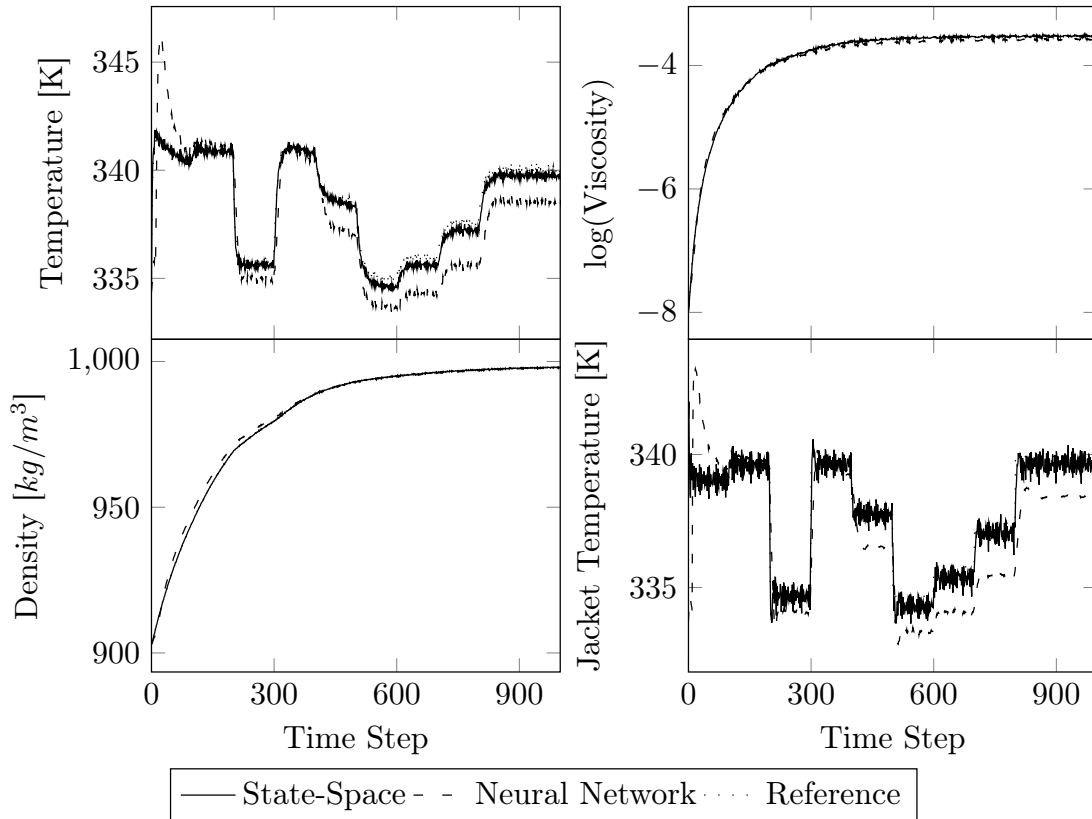


Figure 4.4: Implementation of state-space models and NARX networks into MPC subject to measurement noise and using newly generated reference profiles.

In comparing state-space models and NARX networks, it is worthwhile to not only compare control performance, but also computation times. Table 4.3 tabulates the mean computation times taken for the MPC simulations to complete for each type of model. The total simulation times were averaged over the 30 reference trajectories that were tracked. Since the aim was to evaluate computational complexity, and not performance, $H_p = H_c = 1$ was set as both the prediction and control horizons for the NARX networks in order to make fair comparisons between computation times. Judging by computation time, NARX networks exceeded the state space models in computational complexity by an order of magnitude.

Table 4.3: Mean computation times, in seconds, for MPC simulations.

	Sans Noise	With Noise
State-space	20	21
NARX Network	150	152

Chapter 5

Conclusions and Future Work

The research presented aimed to explore if, in their present state, neural network-based models are a useful tool for process control. In particular, the focus of this study was to compare the efficacy of ANNs with state-space models within the framework of MPC. To this end, state-space and NARX network models were developed for a batch PMMA polymerization process. In this study, subspace-based state-space models outperformed NARX networks in predictive power and control performance. In particular, there was a sizable gap in the prediction capability and control performance with regards to adapting to novel data outside the scope of training data. The NARX networks were found to be vulnerable to over-fitting training data.

The results of this work reveal that NARX networks are worse predictors than state-space models in terms of model-based control. As such, more development is required before neural networks can become viable toward modeling and process control.

Finally, it is to be noted that this study only encompassed NARX networks in the context of a batch PMMA polymerization process, which does not feature highly non-linear behavior and is a single-input multiple-output system. However, there are diverse approaches for leveraging neural networks for the modeling and control of industrial processes. Therefore, future directions for this work include: 1) applying neural network models to the modeling and control of different systems 2) exploring

other neural network architectures, 3) assessing different approaches for implementing neural networks into MPC, 4) increasing process complexity, 5) investigating solutions for addressing over-fitting, and 6) and examining the usefulness of controller performance monitoring in bridging the control performance of NARX networks.

5.1 Different Systems

The PMMA polymerization process that was used as a testbed is a single-input multiple-output system. For future work, it would be worthwhile to examine the viability of neural networks for processes of different complexity. For instance, one can begin by assessing the usefulness of neural networks in the modeling and control of single-input single-output systems. Later, research should be extended to studying the modeling and control performance of neural networks with respect to multiple-input multiple-output systems. In this manner, we will be able to more comprehensively gauge the effectiveness of neural networks, and their possible issues with overfitting, with regards to control problems of varying complexity.

5.2 Different Neural Network Architectures

As previously discussed in Chapter 2, NARX networks are only one choice for the architecture of neural networks. Consequently, it is worth considering the implementation of other architectures to thoroughly review the potential of neural networks for modeling and control applications. For instance, a detailed case study of LSTM networks may be a worthwhile pursuit for future work.

5.3 Other Methodologies

Besides other architectures, there also exist different approaches for implementing ANNs into MPC. For instance, it is possible to predict based on having the inputs to the ANNs encompass the entire historical sequence rather than the most recent data points. Moreover, rather than embedding them into MPC, the ANNs themselves could form the controllers instead. Finally, as inspired by [16], it is possible to consider a hybrid parallel model that employs an ANN, which is auxiliary to the state space model, that models the residual gap between the plant and state-space model. Therefore, there exist other methodologies for applying ANNs toward process control that should be investigated further in subsequent studies.

5.4 Process Complexity

Unlike state-space models, NARX networks are able to directly encode non-linear elements and dynamics. Therefore, a clear advantage of NARX networks is in their ability to handle highly non-linear behaviour. As such, future work should compare state-space models and NARX networks in exceedingly non-linear and complex process dynamics. This will allow for a more comprehensive exploration of the strengths and weaknesses of the two approaches.

5.5 Solutions for Addressing Over-fitting

Besides reducing model complexity, several regularization techniques have been proposed as a means of curtailing the problem of over-fitting, as has been reported previously [30]. However, the value of these regularization techniques for reducing

over-fitting in ANNs that model dynamic processes requires further exploration. As such, applying regularization techniques to the NARX networks identified in this work would comprise a natural continuation to the present study.

5.6 Controller Performance Monitoring

The results of this study show that NARX networks, in comparison with state-space models, were poor predictors of input/output data that are characteristically distinct from the training data. Therefore, it would be prudent to explore the usefulness of controller performance monitoring for evaluating the performance of ANNs in model-based control toward bridging the gap of NARX networks in adapting to novel data.

References

- [1] ABIODUN, O. I., JANTAN, A., OMOLARA, A. E., DADA, K. V., MOHAMED, N. A., AND ARSHAD, H. (2018). State-of-the-art in artificial neural network applications: A survey. *Heliyon*, **4**(11), e00938.
- [2] AGYEMAN, B. T., SAHOO, S. R., LIU, J., AND SHAH, S. L. (2021). LSTM-based model predictive control with discrete inputs for irrigation scheduling. *arXiv preprint arXiv:2112.06352*, .
- [3] ÅKESSON, B. M. AND TOIVONEN, H. T. (2006). A neural network model predictive controller. *Journal of Process Control*, **16**(9), 937–946.
- [4] ALHAJERI, M. S., LUO, J., WU, Z., ALBALAWI, F., AND CHRISTOFIDES, P. D. (2022). Process structure-based recurrent neural network modeling for predictive control: A comparative study. *Chemical Engineering Research and Design*, **179**, 77–89.
- [5] ARDALANI-FARSA, M. AND ZOLFAGHARI, S. (2010). Chaotic time series prediction with residual analysis method using hybrid Elman–NARX neural networks. *Neurocomputing*, **73**(13-15), 2540–2553.
- [6] BENGIO, Y. (2012). Practical recommendations for gradient-based training of deep architectures. In *Neural networks: Tricks of the trade*, pp. 437–478. Springer.
- [7] CORBETT, B., MACDONALD, B., AND MHASKAR, P. (2014). Model predictive quality control of polymethyl methacrylate. *IEEE Transactions on Control Systems Technology*, **23**(2), 687–692.

- [8] CORBETT, B. AND MHASKAR, P. (2016). Subspace identification for data-driven modeling and quality control of batch processes. *AIChE Journal*, **62**(5), 1581–1601.
- [9] DAVE, V. S. AND DUTTA, K. (2014). Neural network based models for software effort estimation: a review. *Artificial Intelligence Review*, **42**(2), 295–307.
- [10] DEBNATH, S., SAHOO, S. R., AGYEMAN, B. T., AND LIU, J. (2023). Input-Output Selection for LSTM-Based Reduced-Order State Estimator Design. *Mathematics*, **11**(2), 400.
- [11] DREISEITL, S. AND OHNO-MACHADO, L. (2002). Logistic regression and artificial neural network classification models: a methodology review. *Journal of biomedical informatics*, **35**(5-6), 352–359.
- [12] EKPO, E. AND MUJTABA, I. M. (2008). Evaluation of neural networks-based controllers in batch polymerisation of methyl methacrylate. *Neurocomputing*, **71**(7-9), 1401–1412.
- [13] FAN, S., GRETTON-WATSON, S., STEINKE, J., AND ALPAY, E. (2003). Polymerisation of methyl methacrylate in a pilot-scale tubular reactor: modelling and experimental studies. *Chemical engineering science*, **58**(12), 2479–2490.
- [14] FAVOREEL, W., DE MOOR, B., AND VAN OVERSCHEE, P. (2000). Subspace state space system identification for industrial processes. *Journal of process control*, **10**(2-3), 149–155.
- [15] GELADI, P. AND KOWALSKI, B. R. (1986). Partial least-squares regression: a tutorial. *Analytica chimica acta*, **185**, 1–17.
- [16] GHOSH, D., MOREIRA, J., AND MHASKAR, P. (2021). Model predictive control embedding a parallel hybrid modeling strategy. *Industrial & Engineering Chemistry Research*, **60**(6), 2547–2562.

- [17] HASSANPOUR, H., CORBETT, B., AND MHASKAR, P. (2020). Integrating dynamic neural network models with principal component analysis for adaptive model predictive control. *Chemical Engineering Research and Design*, **161**, 26–37.
- [18] HEDJAR, R. (2013). Adaptive neural network model predictive control. *International Journal of Innovative Computing, Information and Control*, **9**(3), 1245–1257.
- [19] HOCHREITER, S. AND SCHMIDHUBER, J. (1997). Long short-term memory. *Neural computation*, **9**(8), 1735–1780.
- [20] HOSEN, M. A., HUSSAIN, M. A., AND MJALLI, F. S. (2011). Control of polystyrene batch reactors using neural network based model predictive control (NNMPC): An experimental investigation. *Control Engineering Practice*, **19**(5), 454–467.
- [21] HUANG, Z., LIU, Q., LIU, J., AND HUANG, B. (2022). A comparative study of model approximation methods applied to economic MPC. *The Canadian Journal of Chemical Engineering*, **100**(8), 1676–1702.
- [22] HUNT, K. J., SBARBARO, D., ŻBIKOWSKI, R., AND GAWTHROP, P. J. (1992). Neural networks for control systems—a survey. *Automatica*, **28**(6), 1083–1112.
- [23] JOSEPH, B. AND HANRATTY, F. W. (1993). Predictive control of quality in a batch manufacturing process using artificial neural network models. *Industrial & engineering chemistry research*, **32**(9), 1951–1961.
- [24] KUMAR, S. S. P., TULSYAN, A., GOPALUNI, B., AND LOEWEN, P. (2018). A deep learning architecture for predictive control. *IFAC-PapersOnLine*, **51**(18), 512–517.
- [25] LAVRUKHIN, E. V., GERKE, K. M., ROMANENKO, K. A., ABROSIMOV, K. N., AND KARSANINA, M. V. (2021). Assessing the fidelity of neural network-

- based segmentation of soil XCT images based on pore-scale modelling of saturated flow properties. *Soil and Tillage Research*, **209**, 104942.
- [26] MADHYASTHA, P. AND JAIN, R. (2019). On model stability as a function of random seed. *arXiv preprint arXiv:1909.10447*, .
- [27] MOONEN, M., DE MOOR, B., VANDENBERGHE, L., AND VANDEWALLE, J. (1989). On-and off-line identification of linear state-space models. *International Journal of Control*, **49**(1), 219–232.
- [28] NG, C. AND HUSSAIN, M. A. (2004). Hybrid neural network—prior knowledge model in temperature control of a semi-batch polymerization process. *Chemical Engineering and Processing: Process Intensification*, **43**(4), 559–570.
- [29] NIELSEN, M. A. (2015). *Neural networks and deep learning*, Vol. 2018. Determination press San Francisco, CA.
- [30] NUSRAT, I. AND JANG, S.-B. (2018). A comparison of regularization techniques in deep neural networks. *Symmetry*, **10**(11), 648.
- [31] PSICHOGIOS, D. C. AND UNGAR, L. H. (1992). A hybrid neural network-first principles approach to process modeling. *AIChE Journal*, **38**(10), 1499–1511.
- [32] RHO, H.-J., HUH, Y.-J., AND RHEE, H.-K. (1998). Application of adaptive model-predictive control to a batch MMA polymerization reactor. *Chemical Engineering Science*, **53**(21), 3729–3739.
- [33] SIEGELMANN, H. T., HORNE, B. G., AND GILES, C. L. (1997). Computational capabilities of recurrent NARX neural networks. *IEEE Transactions on Systems, Man, and Cybernetics, Part B (Cybernetics)*, **27**(2), 208–215.
- [34] SUNDERMEYER, M., SCHLÜTER, R., AND NEY, H. (2012). LSTM neural networks for language modeling. In *Thirteenth annual conference of the international speech communication association*.

- [35] TSEN, A. Y.-D., JANG, S. S., WONG, D. S. H., AND JOSEPH, B. (1996). Predictive control of quality in batch polymerization using hybrid ANN models. *AIChE Journal*, **42**(2), 455–465.
- [36] WANG, K., GOPALUNI, R. B., CHEN, J., AND SONG, Z. (2018). Deep learning of complex batch process data and its application on quality prediction. *IEEE Transactions on Industrial Informatics*, **16**(12), 7233–7242.
- [37] WANG, Y., VELSWAMY, K., AND HUANG, B. (2017). A long-short term memory recurrent neural network based reinforcement learning controller for office heating ventilation and air conditioning systems. *Processes*, **5**(3), 46.
- [38] WILLIS, M., DI MASSIMO, C., MONTAGUE, G., THAM, M., AND MORRIS, A. (1991). Artificial neural networks in process engineering. In *IEE proceedings D (control theory and applications)*, Vol. 138, pp. 256–266. IET.
- [39] WU, Z., RINCON, D., AND CHRISTOFIDES, P. D. (2020). Process structure-based recurrent neural network modeling for model predictive control of nonlinear processes. *Journal of Process Control*, **89**, 74–84.
- [40] WUNSCH, A., LIESCH, T., AND BRODA, S. (2021). Groundwater level forecasting with artificial neural networks: a comparison of long short-term memory (LSTM), convolutional neural networks (CNNs), and non-linear autoregressive networks with exogenous input (NARX). *Hydrology and Earth System Sciences*, **25**(3), 1671–1687.
- [41] ZHANG, J. (2005). A neural network-based strategy for the integrated batch-to-batch control and within-batch control of batch processes. *Transactions of the Institute of Measurement and Control*, **27**(5), 391–410.

